Supplementary Information

In situ investigation of ion exchange membranes reveals that ion transfer in hybrid liquid/gas electrolyzers is mediated by diffusion, not electromigration

Maryline Ralaiarisoa[1], Senapati Sri Krishnamurti[1], Wenqing Gu[1], Claudio Ampelli[2], Roel van de Krol[1,3], Fatwa F. Abdi[1], Marco Favaro*[1]*

1) Institute for Solar Fuels, Helmholtz-Zentrum Berlin für Materialien und Energy GmbH, Hahn-Meitner-Platz 14109 Berlin, Germany.

2) Department of Chemical, Biological, Pharmaceutical and Environmental Sciences (ChiBioFarAm), University of Messina, ERIC aisbl and CASPE/INSTM, Messina, Italy.

3) Institut für Chemie, Technische Universität Berlin, Straße des 17. Juni 124, 10623 Berlin, Germany.

*Correspondence and requests for materials should be addressed to: M. Favaro (marco.favaro@helmholtz-berlin.de) and F. F. Abdi (fatwa.abdi@helmholtz-berlin.de).
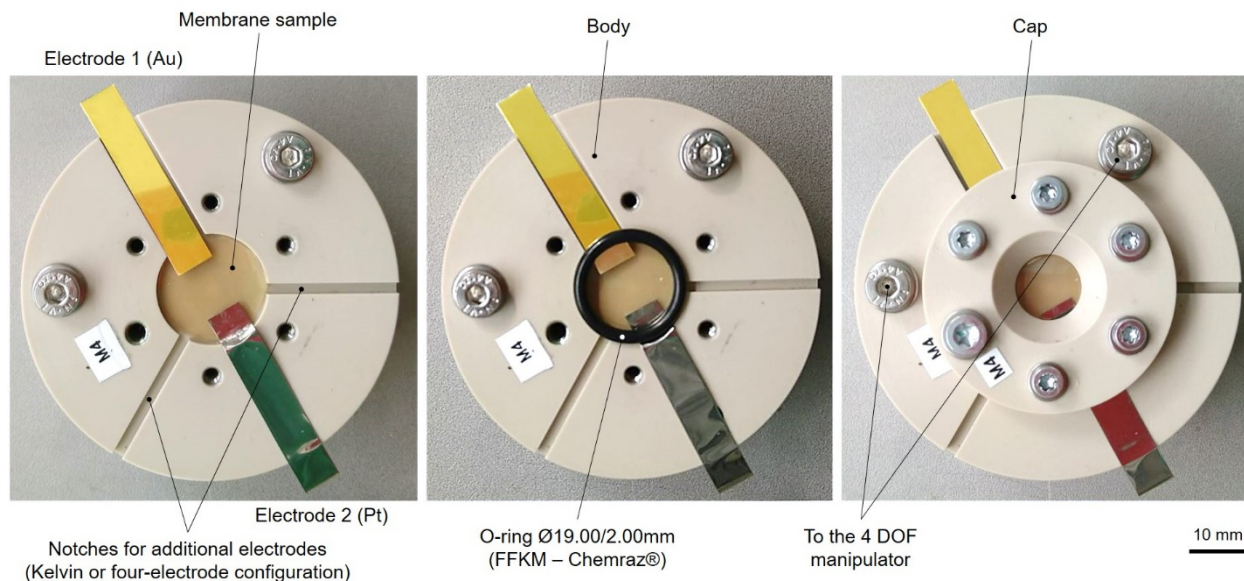
Figure S1. a) Membrane holder used to characterize polymer membranes by means of AP-HAXPES at the SpAnTeX end-station under different environments. Electrical polarization of the membrane sample is also possible. See the experimental section for further details (DOF: degrees of freedom).
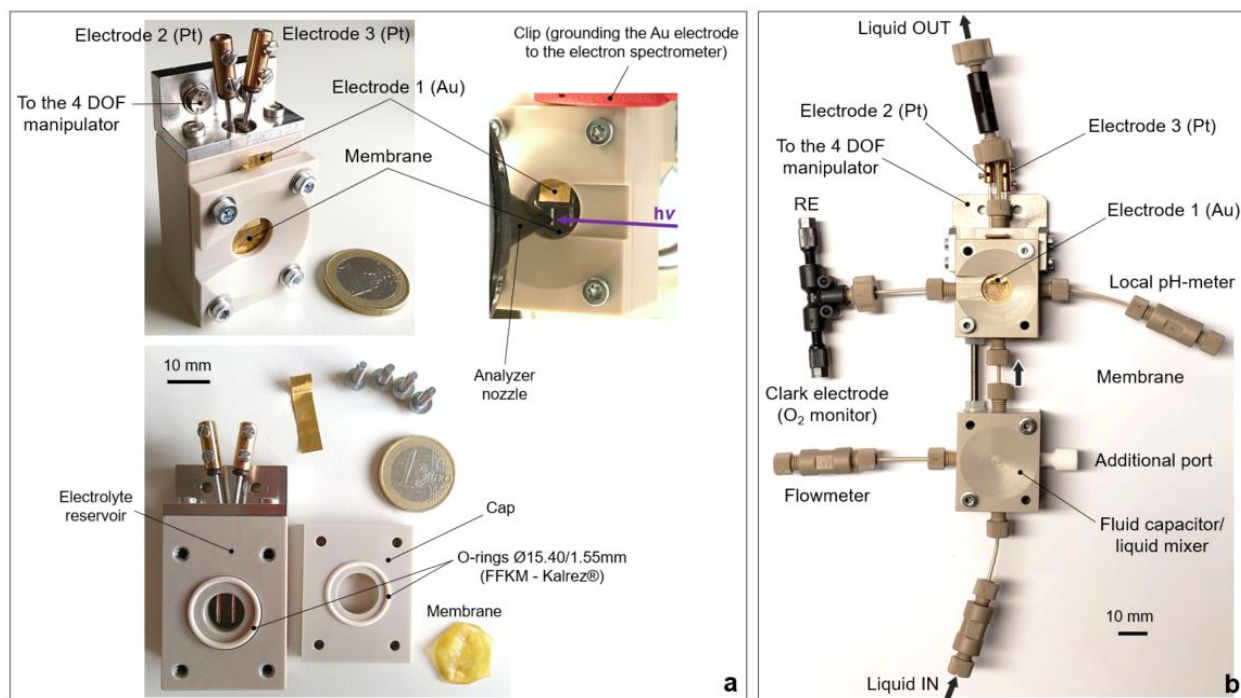

Figure S2. *In situ* static (**a**) and flow (**b**) electrochemical cells used for the *in situ* AP-HAXPES characterization of polymer membranes at the SpAnTeX end-station. The static cell (**a**) was used in this work. The polymer membrane is placed between the cap and the electrolyte reservoir, with FFKM O-rings ensuring the tightness of cell. For the *in situ* flow electrochemical cell (**b**), the liquid electrolyte is pumped from an

external reservoir to the cell mounted in the analysis chamber via a liquid feedthrough using a six-rotor peristaltic pump, allowing the possibility to flow and recirculate the electrolyte. Flow rates range from 1ml/min up to 50 ml/min, in steps of 0.5 ml/min. See the experimental section for further details. DOF: degrees of freedom.
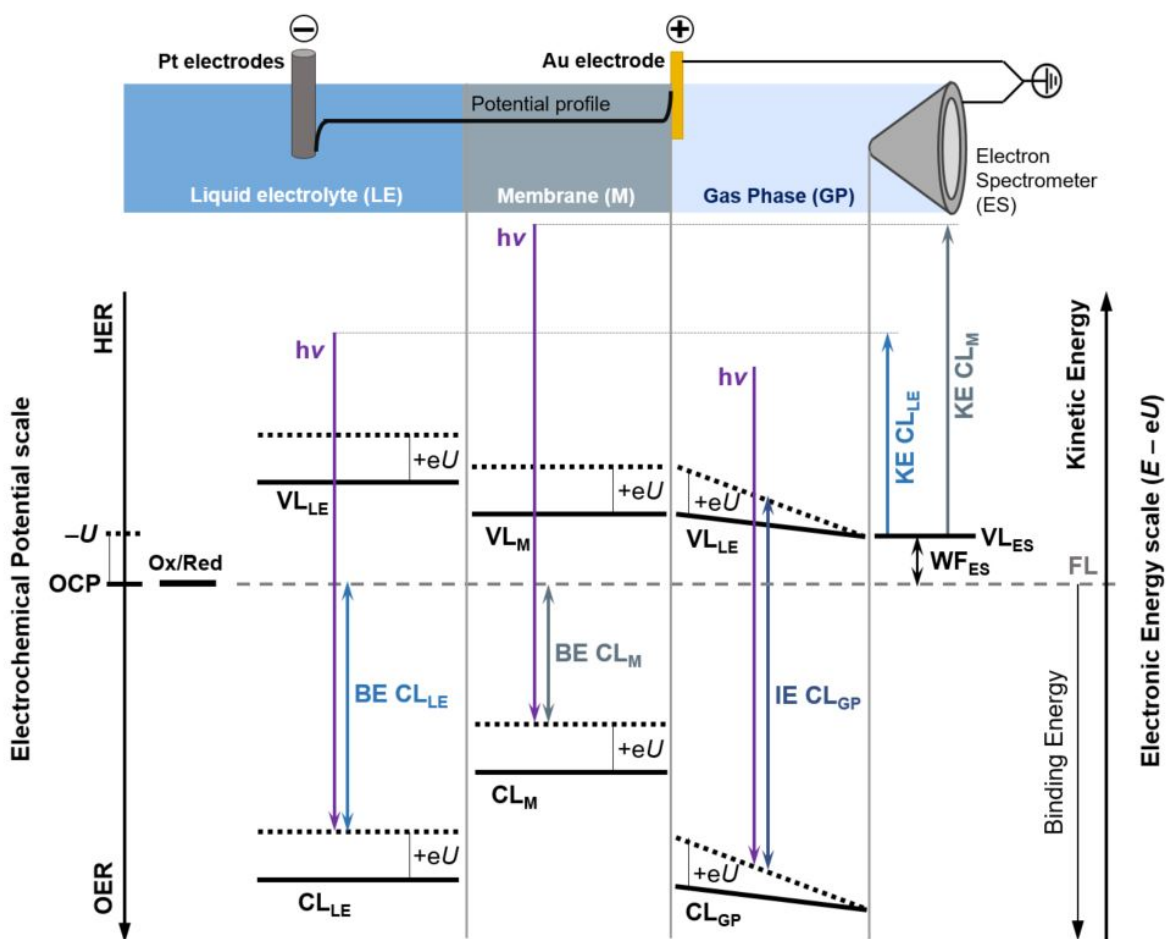
Figure S3. Schematic diagram (not on scale) describing the energy levels for the hybrid liquid/gas electrolyzer in a two-electrode configuration at the half-cell open circuit potential (OCP, solid lines) and under a formal potential of $+U$ ($-U$) applied to the Au (Pt) electrode (dotted lines). The Au electrode, the potentiostat ground, and the electron spectrometer are commonly grounded via a star (Y) connection. The membrane undergoes an electrical polarization, therefore the photoelectrons ejected from the membrane near surface region will experience an increase in kinetic energy passing from OCP to $+U$ ($-U$) applied to the Au (Pt) electrode, corresponding to an apparent core energy level shift by $+eU$ closer to the electron spectrometer Fermi level. Note that electrical double layer effects on the energy level shift in proximity of the metal electrodes are not taken into account. HER: Hydrogen Evolution Reaction; OER: Oxygen Evolution Reaction; VL: Vacuum Level; CL: Core Level; FL: Fermi Level.
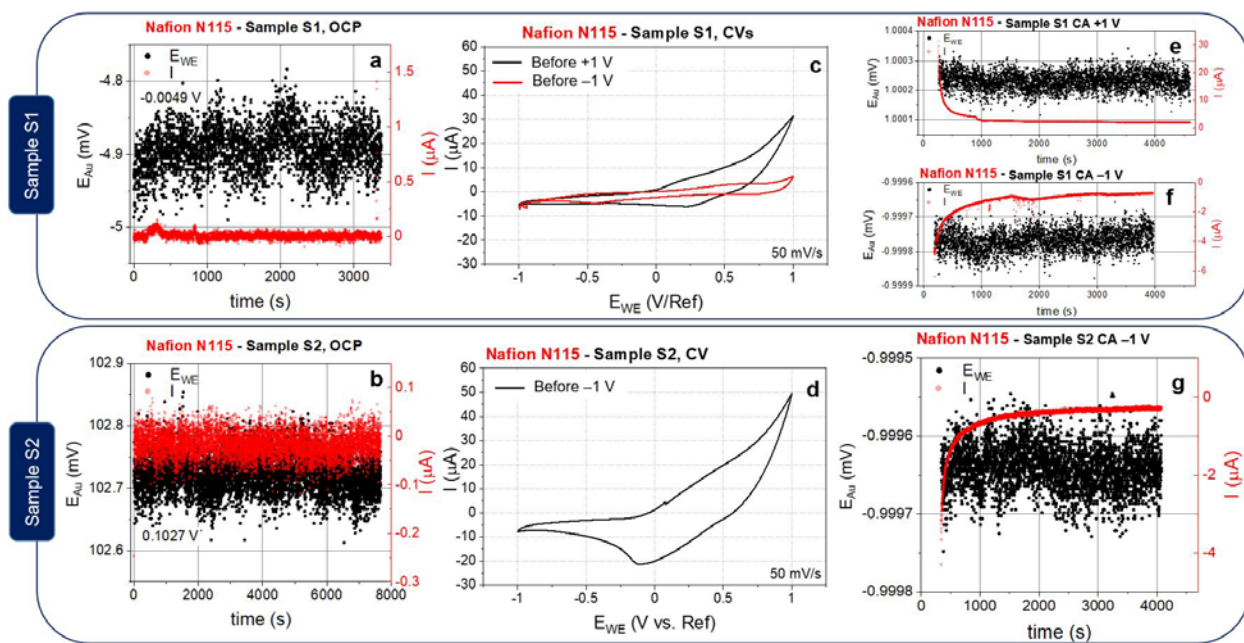
Figure S4. a, b) OCP data and corresponding current during *in situ* AP-HAXPES measurements on samples S1 and S2, respectively (Nafion® N115); **c, d**) Cyclic voltammograms (CV) acquired before applying the targeted potential for S1 and S2, respectively. Chronoamperometry measurements taken during the *in situ* AP-HAXPES experiments at +1 V (**e**) and –1 V (**f**) for sample S1, and at –1 V for sample S2 (**g**). For sample S1, –1 V was applied immediately after the application of +1 V. Note the hybrid liquid/gas electrolyzer was operated as a two-electrode cell. The reported potentials have been applied to the Au electrode contacting the membrane, serving as the working electrode of the cell.
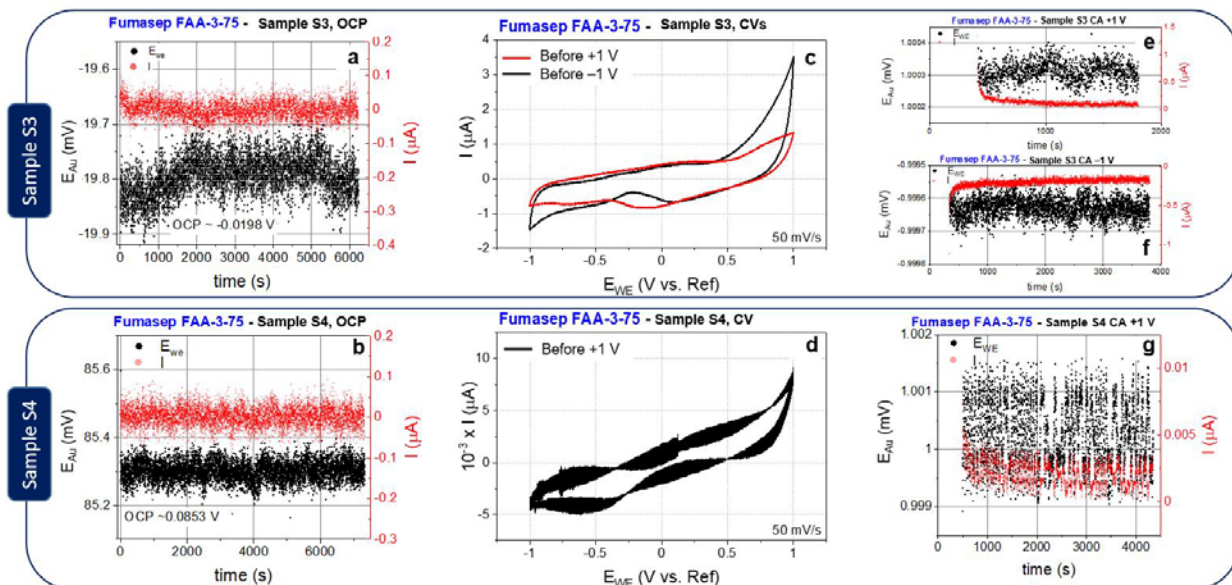
Figure S5. a, b) OCP data and corresponding current during *in situ* AP-HAXPES measurements on samples S3 and S4, respectively (Fumasep® FAA-3-75); **c, d**) Cyclic voltammograms (CV) acquired before applying the targeted potential for S1 and S2, respectively. Chronoamperometry measurements taken during the *in situ* AP-HAXPES experiments at +1 V (**e**) for sample S3, and at +1 V (**f**) and 1 V (**g**) for sample S4. For the latter, –1 V was applied immediately after the application of –1 V. Note the hybrid liquid/gas electrolyzer was operated as a two-electrode cell. The reported potentials have been applied to the Au electrode contacting the membrane, serving as the working electrode of the cell.

**Table S1.** Baseline parameters used in the finite element simulations.

	Parameter	Value	Ref.
Electrolyte	Initial concentration of Na$^+$, $c_{Na^+,0}$	1 M	
	Initial concentration of Cl$^-$, $c_{Cl^-,0}$	1 M	
	Diffusivity of Na$^+$ D_{Na^+}	1.334×10^{-9} m^2/s	1
	Diffusivity of Cl$^-$ D_{Cl^-}	2.032×10^{-9} m^2/s	1
	Density, ρ	1.058 g/L	2
	Electrolyte conductivity, σ_l	8.096 S/m	3
	Temperature, T	293.15 K	
Membrane	Initial concentration of Na$^+$, $c_{Na^+,m,0}$	0 M	
	Initial concentration of Cl$^-$, $c_{Cl^-,m,0}$	0 M	
	Diffusivity of Na$^+$ in Nafion, $D_{Na^+,m}$	1.58×10^{-10} m^2/s	4
	Diffusivity of Cl$^-$ in Nafion, $D_{Cl^-,m}$	1.75×10^{-13} m^2/s	see Section 3.2.3 and 3.3 in the manuscript
	Diffusivity of Na$^+$ in Fumasep, $D_{Na^+,m}$	5.10×10^{-14} m^2/s	see Section 3.2.3 and 3.3 in the manuscript
	Diffusivity of Cl$^-$ in Fumasep, $D_{Cl^-,m}$	2.032×10^{-10} m^2/s	$\dfrac{D_{Cl^-}}{D_{Na^+}} \times D_{Na^+,m=Nafion}$
	Porosity, ε_p	0.05	
	Conductivity of Nafion	0.1 S/cm	5
	Conductivity of Fumasep	0.065 S/cm	6
	Area resistance of Nafion	$0.2\ \Omega \cdot cm^2$	7

	Area resistance of Fumasep	$2\ \Omega \cdot cm^2$	6
Electrode	Exchange current density, j_0	10^{-5} A/m^2	
	Anodic transfer coefficient, α_a	0.5	
	Cathodic transfer coefficient, α_c	0.5	
Geometry	Thickness of Nafion, d_m	127 μm	5
	Thickness of Fumasep, d_m	80 μm	6
	Cell height, h_{cell}	10 mm	
	Electrolyte width, d_{el}	10 mm	

References

1. E. Samson, J. Marchand, K. A. Snyder, Calculation of ionic diffusion coefficients on the basis of migration test results, *Materials and Structures*, 36, 2003, 156-165.

2. D. Rowland, Advanced Thermodynamics, 2021, online; accessed 2023-03-20 https://advancedthermo.com/electrolytes/density_NaCl.html.

3. F. F. Hervas, P. C. Serra, C. B. Torres, M. P. Fernandez, D. Queralto, J. C. Ribas, J. C. Cosp, A. Marsal, A. Marnich, Study of the extraction kinetic of glycosaminoglycans from raw sheepskin trimmings, 2006. https://iultcs.org/wp-content/uploads/2022/05/V-7-Study-of-the-extraction-kinetic-of-glycosaminoglycans-from-raw-sheepskin-trimmings.pdf

4. I.A. Stenina, Ph. Sistat, A.I. Rebrov, G. Pourcelly, A.B. Yaroslavtsev, Ion Mobility in Nafion-117 membranes, *Desalination*, 170, 2004, 49-57.

5. Nafion[TM] N115, N117, N1110, http://fuelcellearth.com/pdf/nafion-N115-N117-N1110.pdf, accessed 2023-03-20.

6. Fumasep[®] FAA-3-PK-75, https://fuelcellstore.com/spec-sheets/fumasep-faa-3-pk-75-technical-specifications.pdf, accessed 2023-03-20.

7. K. Weißhaar, Modifizierung und Charakterisierung der Membran- und Elektrodenmaterialien der Vanadium-Redox-Flow-Batterie. Universität des Saarlandes, **2018**. https://doi.org/10.22028/D291-27862.
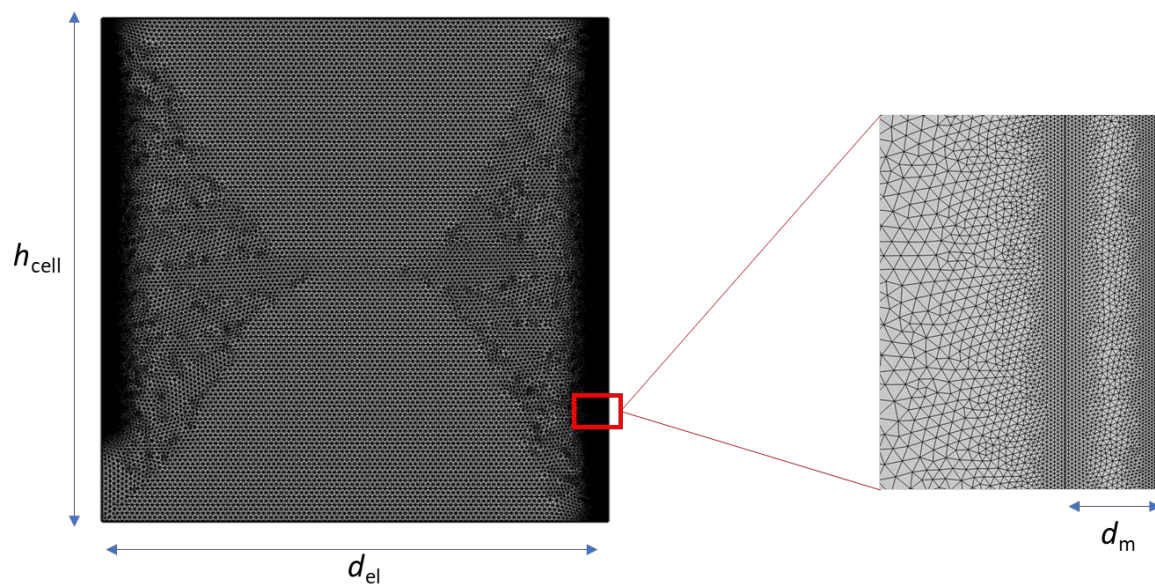
Figure S6. Mesh configuration used in this work for the finite element analysis. h_{cell} = cell height, d_{el} = electrolyte thickness, d_m = membrane thickness.
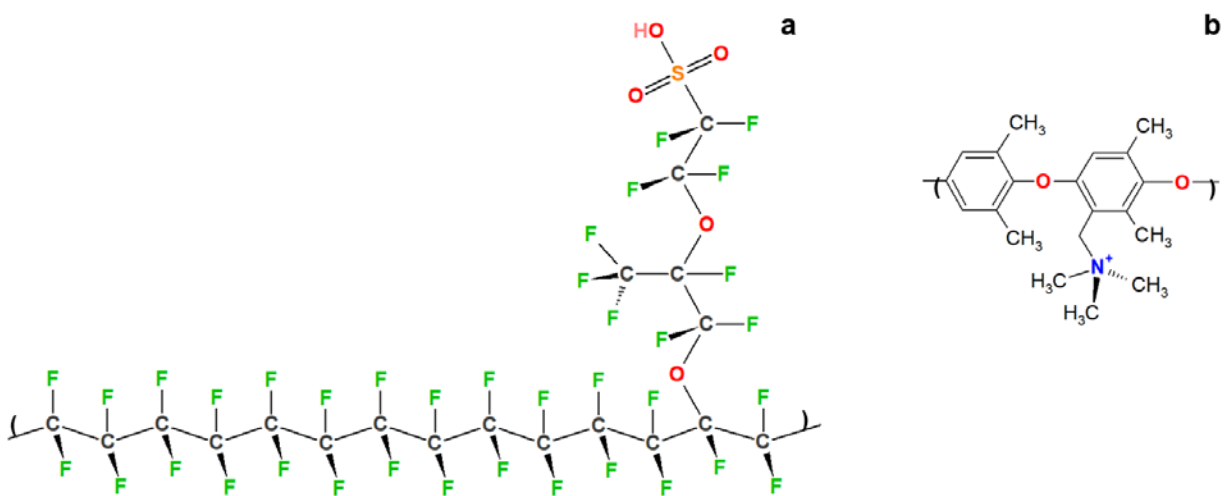
Figure S7. a) Chemical structure of Nafion® 115; **b)** Polyaromatic chemical structure typical of Fumasep® FAA membranes, such as FAA-3-75.

Table S2. Summary of the quantitative analysis based on the spectral fits of the HAXPES data reported in Figure 2 for the Nafion® N115 membrane.

		Experimental	
Ratio	**Nominal**	**at hv = 3000 eV**	**at hv = 6000 eV**
$-CF_2-/CF_2-SO_3^-$	13:1 = 13.0	14.10 (C 1s fitting)	12.56 (C 1s fitting)
$-CF_2-/-OCF-$	13:2 = 6.5	7.59 (C 1s fitting)	7.31 (C 1s fitting)
$-CF_2-/-OCF_2,-CF_3$	13:(2+1) = 4.3	4.21 (C 1s fitting)	4.10 (C 1s fitting)
$-SO_3^-/-CF-O-CF_2-$	3:2 = 1.5	1.50 (O 1s fitting)	-

Table S3. Summary of the quantitative analysis based on the spectral fits of the HAXPES data reported in Figure 2 for the Fumasep® FAA-3-75 membrane.

|		Experimental	
Ratio	**Nominal**	**at hv = 3000 eV**	**at hv = 6000 eV**
sp^2**C** / **C**–N, **C**–O	1.0	1.12 (C 1s fitting)	0.97 (C 1s fitting)
sp^2**C** / sp^3**C**	2.0	0.75 (C 1s fitting)	0.74 (C 1s fitting)
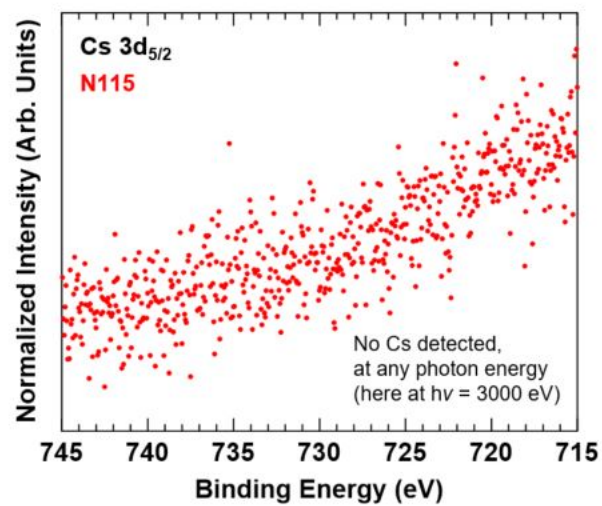
Figure S8. Cs $3d_{5/2}$ core level acquired on Nafion® N115 at hv = 3000 eV.
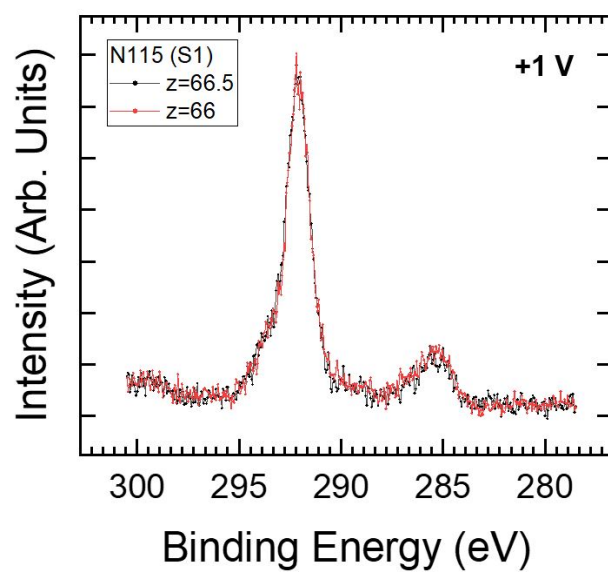

Figure S9. C 1s core level spectra of Nafion® N115 sample S1 under the application of an anodic bias of +1 V at two different positions on the membrane along the vertical axis z (z in mm). The spectra are overlapping, i.e. no BE shift is observed between two different position, indicating that both spots of the same sample are at the same potential.
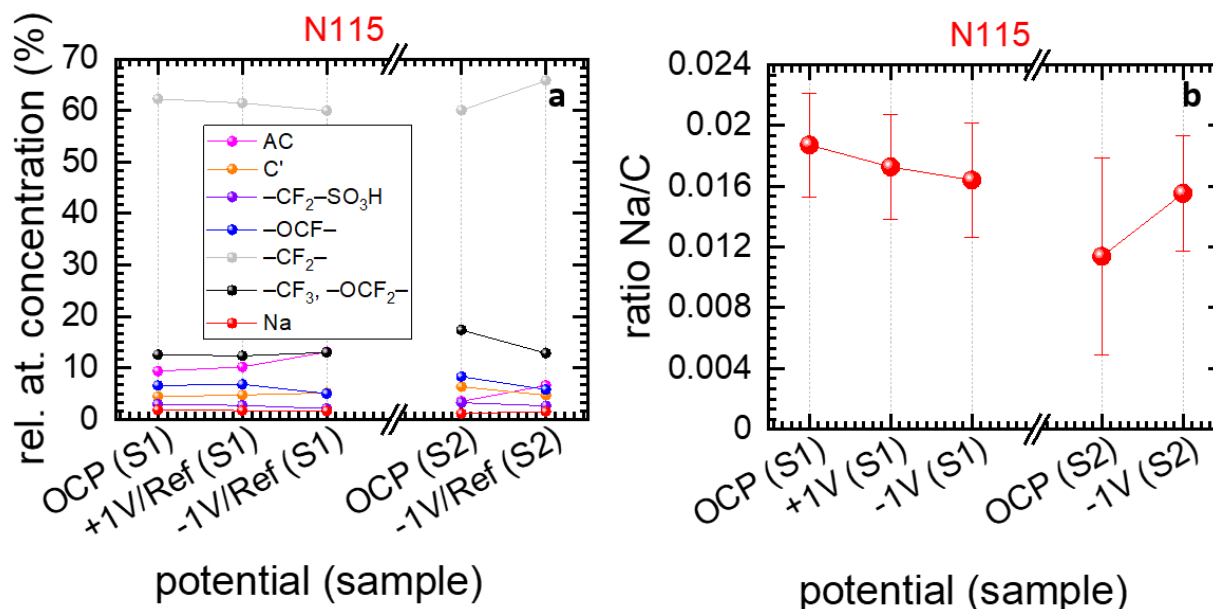
Figure S10. a) Relative atomic concentration of the different carbon spectral contributions extracted from the fits of the core level spectra reported in **Figure 3** for samples S1 and S2; **b)** Na/C ratio, accounting for of all 6 carbon contributions. The error bars indicate that the variation of the reported values here are still within the experimental uncertainty of the measurement. The error bars are obtained following the error evaluation steps reported below.
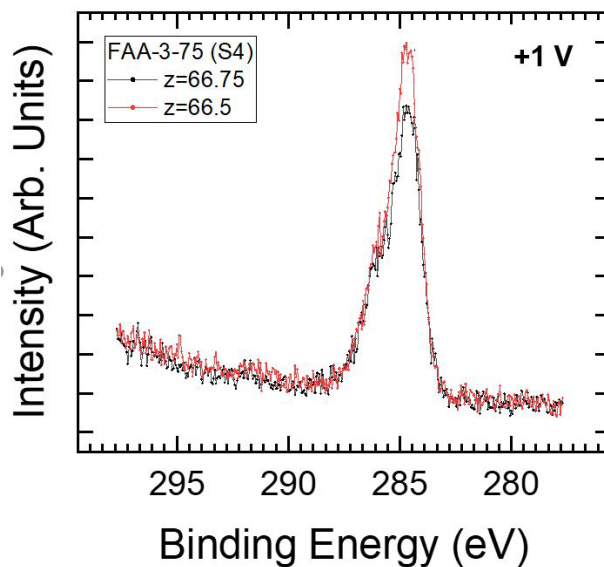
Figure S11. C 1s core level spectra of Fumasep® FAA-3-75 sample S4 under the application of an anodic bias of +1 V at two different positions on the membrane along the vertical axis z (z in mm). The spectra are overlapping, i.e. no BE shift is observed between two different position, indicating that both spots of the same sample are at the same potential.
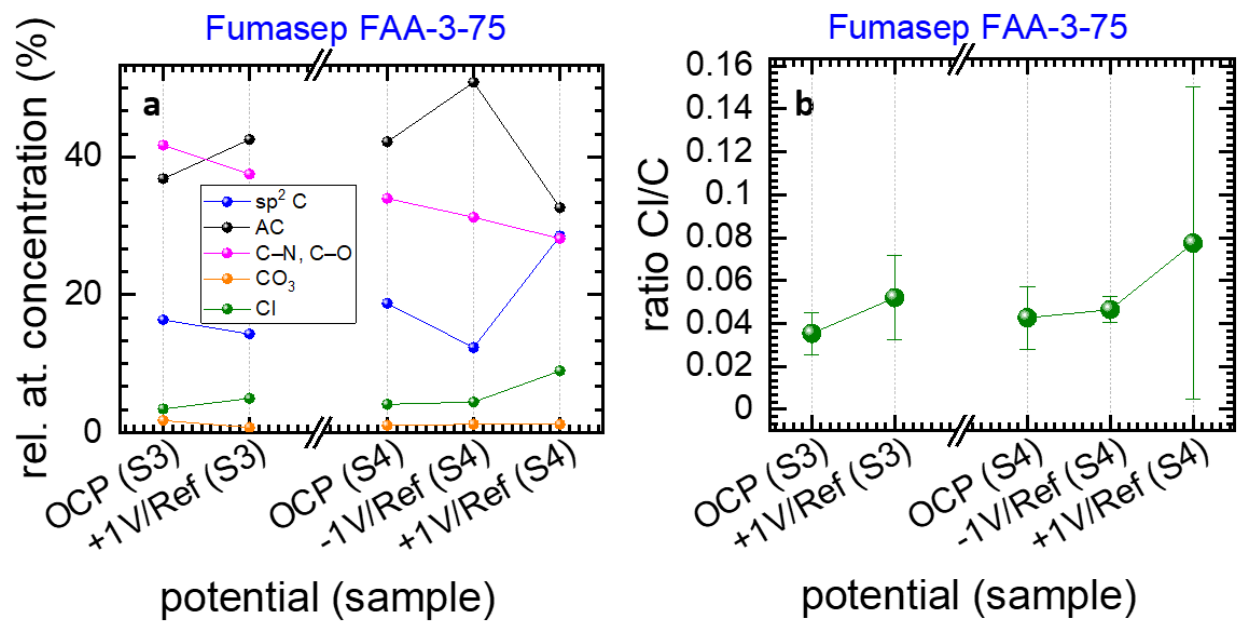
Figure S12. a) Relative atomic concentration of the different carbon spectral contributions extracted from the fits of the core level spectra reported in **Figure 4** for samples S3 and S4; **b)** Cl/C ratio, accounting for of all 4 carbon contributions. The error bars indicate that the variation of the reported values here are still within the experimental uncertainty of the measurement. The error bars are obtained following the error evaluation steps reported below.
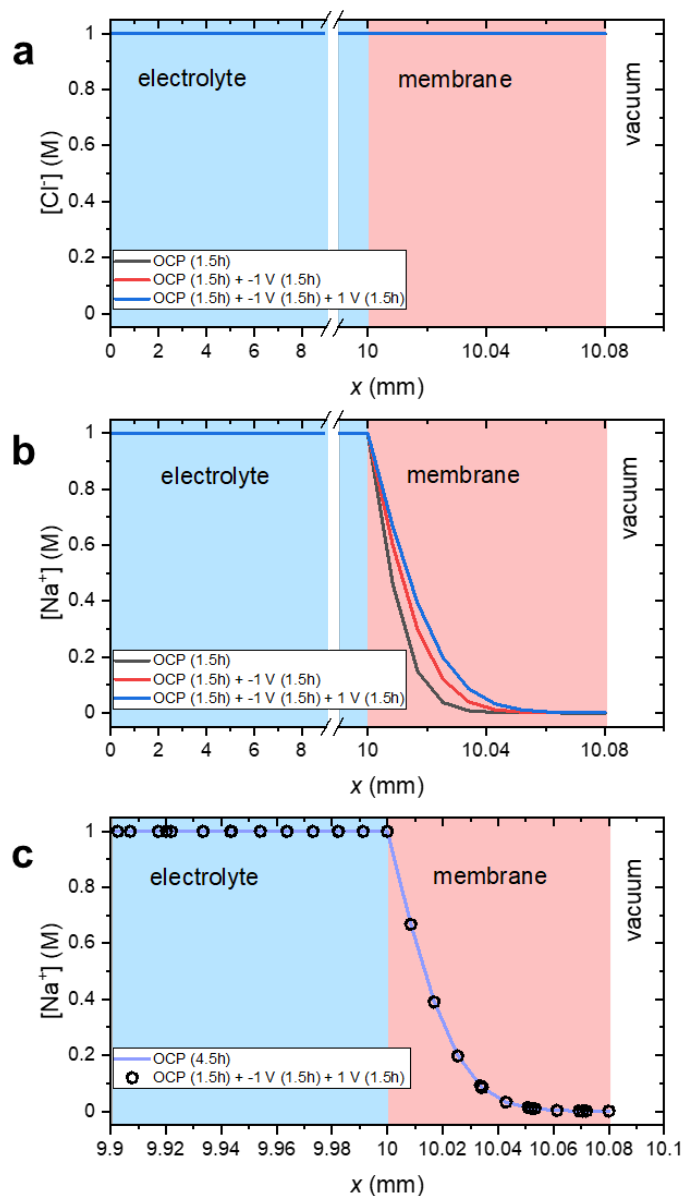
Figure S13. Simulated concentration profile of (**a**) Cl⁻ and (**b**) Na⁺ throughout the electrolyte and FAA-3-75 membrane. Three different electrochemical conditions, based on our AP-HAXPES experiments, were considered: (i) half-cell open circuit potential (OCP) for 1.5 hours, (ii) OCP for 1.5 hours followed by the application of −1 V for 1.5 hours, and (iii) OCP for 1.5 hours followed by the application −1 V for 1.5 hours and +1 V for 1.5 hours. (**c**) Comparison of the simulated concentration profile of Na⁺ at regions close to and inside the Fumasep membrane under the electrochemical condition (iii) above (black circles) and OCP for 4.5 hours (blue line).

Error evaluation:

The relative uncertainty of a measured signal value x is determined as:

$$\sigma_R = \frac{\sigma(x)}{x}$$

where, σ is the standard deviation of the variable x.

For pulse-counting systems, the signal-to-noise ratio S/N determines the uncertainty that gives the error bar in quantification of the peak area of signal intensity S, and background noise N :[1]

$$\sigma_R = \frac{1}{S/N}$$

and:

$$\frac{S}{N} = \frac{P - B}{N(B)}$$

where P, and B represent the peak, and background in an XPS spectrum, respectively. N is the background noise.

To evaluate the error of the fitting data, the signal intensity S=P-B is taken as the difference between the highest intensity (P) from the fit peak of interest and the fitted background intensity (B). We approximate the latter as the average background over a definite region (of n>16 values) on the higher kinetic energy side of the spectrum, about 2 up to 10 eV away from the peak maximum. Furthermore, we evaluate N(B) as the RMS noise of the background as follows:

$$N(B) = \sqrt{\frac{1}{n}\sum_{i=1}^{n}\left((x_i - \hat{x}_i)\right)^2}$$

which estimates the deviation of the experimental values x_i (observed values) from fit values $\hat{x}_i$ (predicted values) of the background within a definite region (of $n > 16$ values) on the higher kinetic energy side of the spectrum, about 2 up to 10 eV away from the peak maximum.

Once the peak area error σ_R is determined, the errors of the quantities (e.g. concentration and ratio) derived from the peak area are determined following the error propagation rules. For the addition of peak area contributions of two species (1,2) of the same element Y, the error is approximated by the relative uncertainty:

$$\sigma_R(Y_1 + Y_2) = \frac{\sigma\,(Y_1 + Y_2)}{A_1 + A_2} = \frac{\sqrt{\sigma^2(Y_1) + \sigma^2(Y_2)}}{A_1 + A_2} = \frac{\sqrt{\left(\sigma_{R,1}(Y_1) \times A_1\right)^2 + \left(\sigma_{R,2}(Y_2) \times A_2\right)^2}}{A_1 + A_2}$$

where σ is the absolute uncertainty, A_i is the fitted peak area (under consideration of the sensitivity factor) of species i. $\sigma_{R,i}(Y_i)$ is the peak area error for species Y_i. For the calculation of peak area ratio of two different elements X_1, and X_2, the error is approximated by the relative uncertainty:

$$\sigma_R\left(\frac{X_1}{X_2}\right) = \sqrt{\sigma_{R,1}^2(X_1) + \sigma_{R,2}^2(X_2)}$$

where $\sigma_{R,1}$ and $\sigma_{R,2}$ are the respective relative uncertainties, i.e. errors, of the peak area of the element X_1, and X_2, respectively.

(1)   Hofmann, S. *Auger- and X-Ray Photoelectron Spectroscopy in Materials Science: A User-Oriented Guide*; Springer Science & Business Media, 2012.